Improvement of bonding strength between Au/Ti and SiO_2 films by Si layer insertion

Hirotoshi Nagata
OptoelectronicS Research Division, New Technology Research laboratories, Sumitomo Osaka Cement Co., Ltd., Fanabashi-shi. Chiba 274-8601. Japan

Takashi Shinriki
Optoelectronics Division, Sumitomo Osaha Cement Co.. Ltd., Fuaabashi-shi. Chiba 274-8601. Japan

Kaori Shima, Masumi Tamai, and Eungi Min Haga
Advanced Materials Research Division, New Tecimology Research Laboratories. Sumitomo Osaka Cement Co., Ltd.. Fuaabashi-shi. Chiba 274-8601. Japan

(Received 23 June 1998; accepted 29 January 1999)

In the fabrication of broad band optical waveguide modulators, a certain technology must be used to prepare 15-20-μm-thick Au electrodes on the SiO_2 surface covering the waveguides. A thin transition metal film is commonly inserted between the Au and SiO_2 to improve adhesive strength. The transition metal film used in this study is Ti. Here, the SiO_2 surface is precoated with Si prior to the Ti film formation, demonstrating a significant improvement in adhesive strength. The Si layer works as a barrier against oxidation of the Ti film due to the SiO_2 , Ieading to a homogenous film growth of metallic Ti. © 1999 American Vacuum Society. [S0734-2101(99)02503-8]

I. INTRODUCTION

Metallization of SiO_2 film surfaces is a key process in the fabrication of electronic and optoelectronic devices, and a higher adhesive strength of metal layers is needed to increase the mechanical reliability of these devices. In this regard, for instance, prior to the formation of an Au electrode layer on SiO_2 coated substrates, transition metal films, such as Ti or Cr, are usually deposited to strongly bind the SiO_2 and Au together.[1] The technique is also applied to the fabrication of $LiNbO_3$ based optical waveguide devices because they need very thick Au electrode layers to achieve a high speed electro-optical response for their use in optical fiber communication systems. [2-4] The $LiNbO_3$ devices consist of a $LiNbO_3$ substrate with Ti-indiffused optical waveguides, an approx. I /hm thick SiO_2 buffer layer covering the substrate, and a 15-20-∝m-thick Au electrode layer. Such a thick Au electrode layer is prepared using electroplating on the SiO_2 previously metallized by a sequential vacuum deposition of a thin transition metal (Ti or Cr) and Au films.

For $LiNbO_3$ devices installed with thick Au electrodes, a greater adhesive strength between the SiO_2 and the metal layers is the key to achieving high device reliability. The peeling of electrodes from the substrate may be due to large internal stress in the thick electrode layer. In our experience, such breaks were found to occur at the Ti layer which had been inserted between vacuum evaporation deposited SiO_2 and Au layers. In order to improve their adhesive strength, first we sought out what caused the film to peel and then the effect of inserting a thin Si layer between SiO_2 and Ti. The Si layer was found to prevent the Ti layer from oxidization during film growth and thus, increase its adhesive strength to the SiO_2 layer.

II. EXPERIMENTAL PROCEDURE

In order to examine the phenomena occurring at the boundary, samples without thick electroplated Au layers were prepared. On the $LiNbO_3$ substrates, a 550-nm-thick SiO_2 film was deposited by a conventional vacuum evaporation technique followed by O_2 atmosphere annealing at 600ϒC for 5 h. On some samples, a 80-nm-thick Si film was deposited at an ambient substrate temperature by conventional radio frequency (rf)-magnetron sputtering of a non-doped Si target with Ar. Then, both samples, with and without the Si layer, were placed in the vacuum evaporation chamber for a sequential deposition of 50-nm-thick Ti and 35-nm-thick Au layers. During the deposition, the substrates were heated to about 200ϒC. The deposition of the Au/Ti binary film on all of the samples was carried out by the same run, in order to make deposition conditions the same, such as back-pressure gases, etc.

These two kinds of samples were evaluated for their adhesive strength and chemical characteristic of layers, especially the Ti layer. The adhesive strength was measured by a scratch tester, in which a diamond stylus, pressed onto the sample, traced the surface while being vibrated at 30 Hz normal to the tracing direction.[5] Then the load applied to the stylus was increased step by step at a magnitude of 0.735 mN/step. As the load increased, the operation voltage necessary to vibrate the stylus also increased and showed abrupt changes when the film began to peel from the sample. [5]

The chemical analyses of the samples were performed using a conventional electron probe microanalyzer (EPMA), a scanning electron microscope (SEM), an x-ray photoelectron spectrometer (XPS), an x-ray diffractometer (XRD), and an atomic force microscope (AFM). In order to examine the Ti layer, some samples were prepared without the Au film ($Ti/Si/SiO_2$ / $LiNbO_3$ and Ti/SiO_2 / $LiNbO_3$ samples).

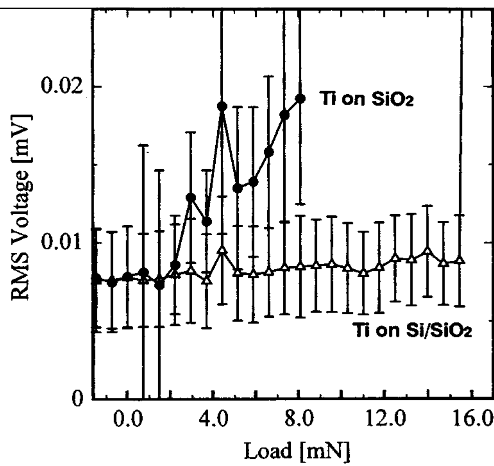

FIG. 1 . Scratch test results for samples with the Si layer (white uiangles) and without the Si (black circles). The horizontal axis denotes the load applied to the stylus contacting the sample suface, and the vertical axis denotes the voltage necessary to vibrate the stylus on the sample.

III. RESULTS AND DISCUSSION

A. Adhesive Strength

Figure I shows the scratch test results of the samples with the Si layer (white triangles) and without the Si (black circles). The horizontal axis denotes the load applied to the stylus, and the vertical axis denotes the voltage necessary to vibrate the stylus on the sample. For the sample with Si the voltage necessary to vibrate the stylus rose gradually with increasing load, and at the 15.4 mN Ioad, jumped abruptly

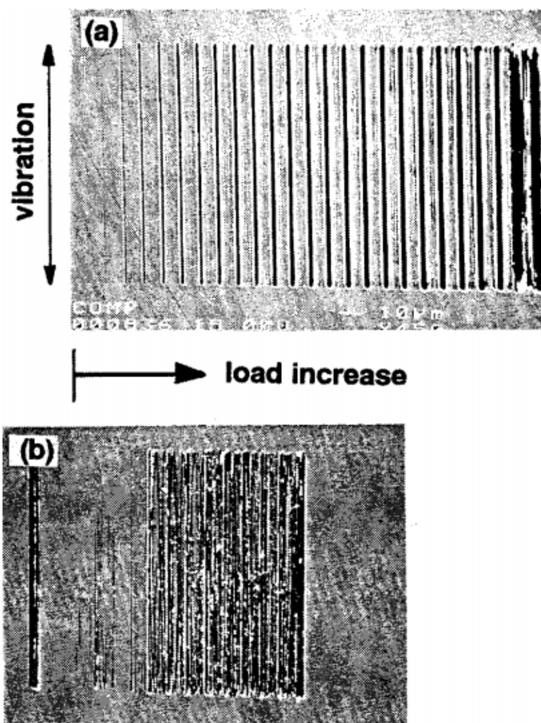

FIG. 2. SEM images of surface flaws on the samples with Si (a) and without Si (b) atter the scratch tests. A gap bctween fiaw marks is about 10 μm.

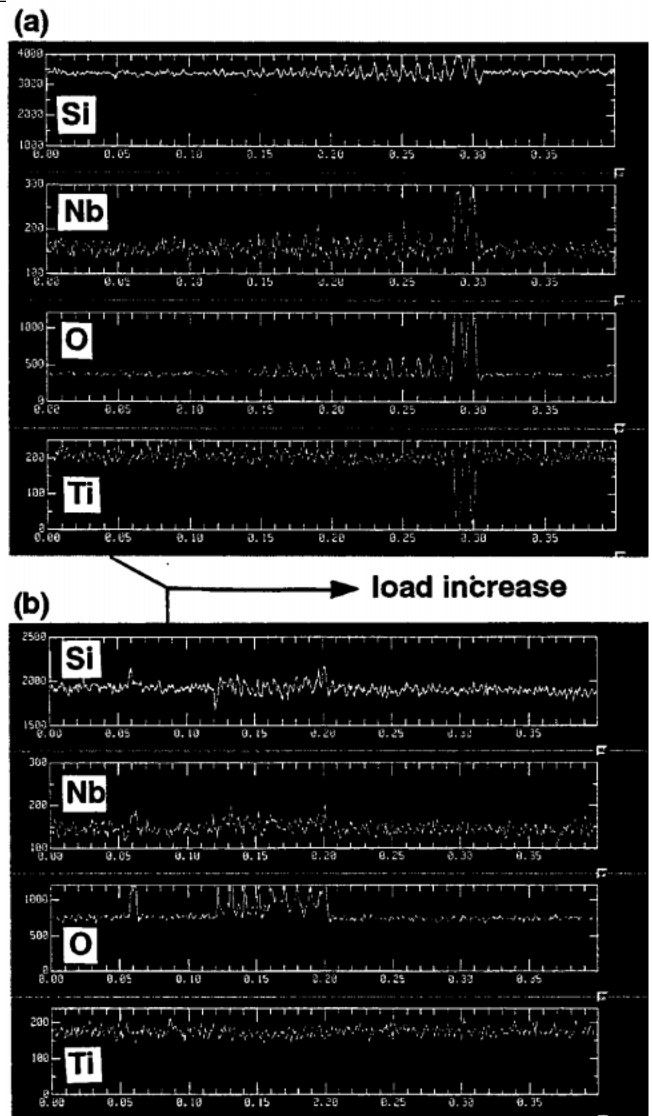

FIG. 3. EPMA results measured along the direction in which the applied load increased in Fig. 2: (a) for the sample with Si and (b) for the sample without Si. The venical and horizontal axes denote the detected intensity of the elements and the measurement position on the sample surface, respectively.

because the stylus scratched out the surface layers. However, data for the sample without Si was clearly different; the voltage necessary to vibrate the stylus increased extraordinarily at just the 2.9 mN Ioad. These results revealed that the surface layers of the sample without Si could be scratched out by the stylus with only one fifth of the load it took for the sample with Si.

In order to examine the position of the break in the surface layers, the tested samples were analyzed by SEM and EPMA. Figure 2 reveals SEM images of surface flaws on the sample with Si (a) and without Si (b) after the scratch tests. Figures 3(a) and 3(b) are the corresponding EPMA results measured along the direction in which the applied load increased. The EPMA measurements were performed for Si, Nb, O, and Ti elements, and the vertical and horizontal axes of Fig. 3 denote the detected intensity of the elements and the measurement position on the sample surface, respec-

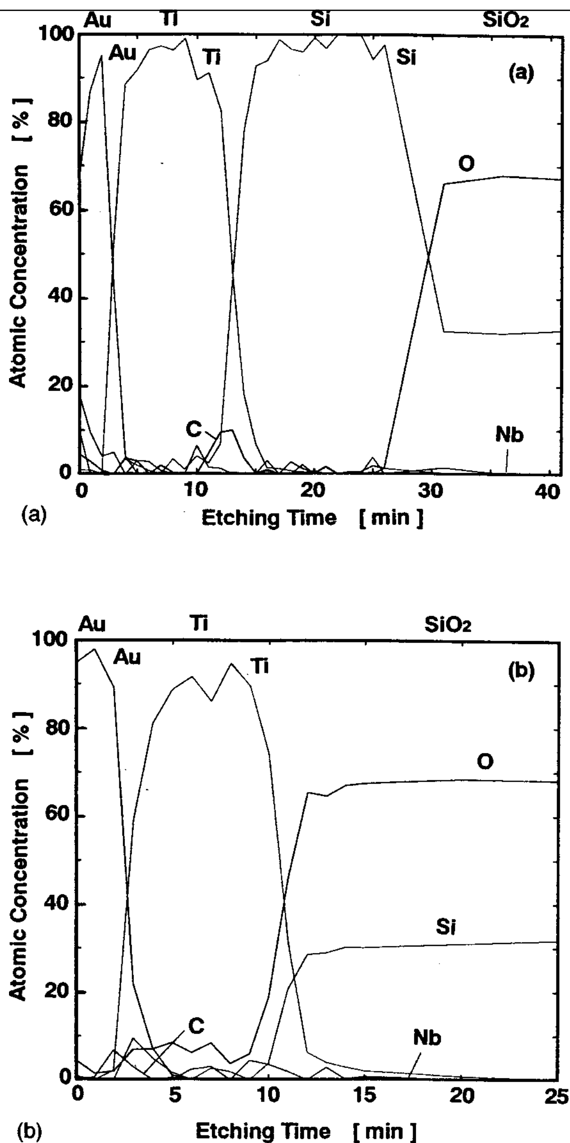

FIG. 4. XPS depth profiles for the samples: (a) for the sample with Si and (b) for the sample without Si.

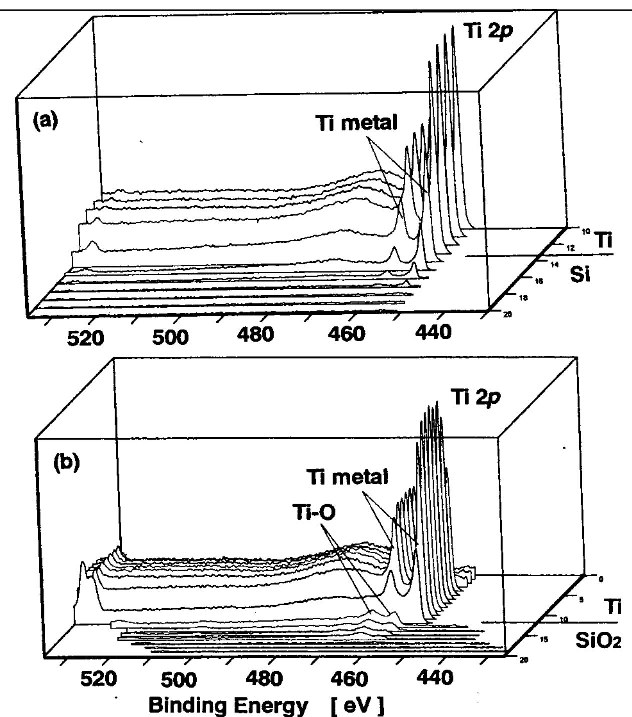

FIG. 5. XPS spectra for Ti $2p$ near the boundary between (a) Ti and Si layers and (b) Ti and SiO_2 layers. The horizontal axis denotes the measured binding energy which was calibrated using a certain C $1s$ peak energy.

tively. Similar to the results of Fig. 1 , a significant difference was observed in the morphology of the scratched surface depending on the existence or absence of the Si interlayer. In the sample with Si, the depth of the scratch was increased gradually along with the increased load applied to the stylus as shown in Figs. 2(a) and 3(a). In particular, the intensity of Si and O signals in Fig. 3(a), coming from the Si/SiO_2 binary layer under the metal layers, grew steadily with increasing load, indicating that the Au/Ti binary layer kept a firm adhesion to the SiO_2 • At the critical load (15.4 mN in Fig. l), however, the metal films were completely scratched out, causing an emergence of the Nb signal from the $LiNbO_3$ substrate under the SiO_2 Iayer and an absence of the Ti signal. Judging from the significantly great intensity of the Nb and O signals, there is a possibility that the SiO_2 Iayer was also partially scratched out along with the Aurri/Si layers at this load level.

Concerning the no-Si sample, as shown in Fig. 2(b), the surface crumbled when a certain load was applied to the vibrating stylus. This critical load corresponded to the value of 2.9 mN in Fig. I at which the voltage needed to vibrate the stylus began to increase. The corresponding EPMA results showed large O signals and weak signals of Si and Nb, suggesting that, at the very least, the Au/Ti layers were completely broken. In other words, the adhesive strength of the Ti film to the SiO_2 Iayer was evidently weaker than that of the Ti film to the Si precoated SiO_2 Iayer. Furthennore, this Ti film seemed to be more fragile compared with the Ti on the Si/SiO_2 Iayer.

The above results proved that the existence of the thin Si layer on the SiO_2 films affected the mechanical characteristics of the deposited Ti layer. To maintain the high adhesive strength of the top Au layer, especially Au electrodes over the device surfaces, insenion of an Si layer between the Ti and SiO_2 was found to be effective. Observed differences in the Ti layer characteristics are discussed in the following sections from viewpoints of chemical and physical structures.

B. Chemical Structure

Figures 4(a) and 4(b) show XPS depth profiles of samples with and without the Si layer, respectively. In the XPS measurements, intensities of photoelectron signals for Au $4f$, Ti $2p$, Si $2p$, O Is, C Is, and Nb $3d$ were monitored while each sample surface was etched by irradiation of Ar ions in the analyzer chamber. In order to examine the chemical structures of mainly the Ti layer, the Ar ion etching was carried out until the SiO_2 Iayer appeared. The vertical and horizontal

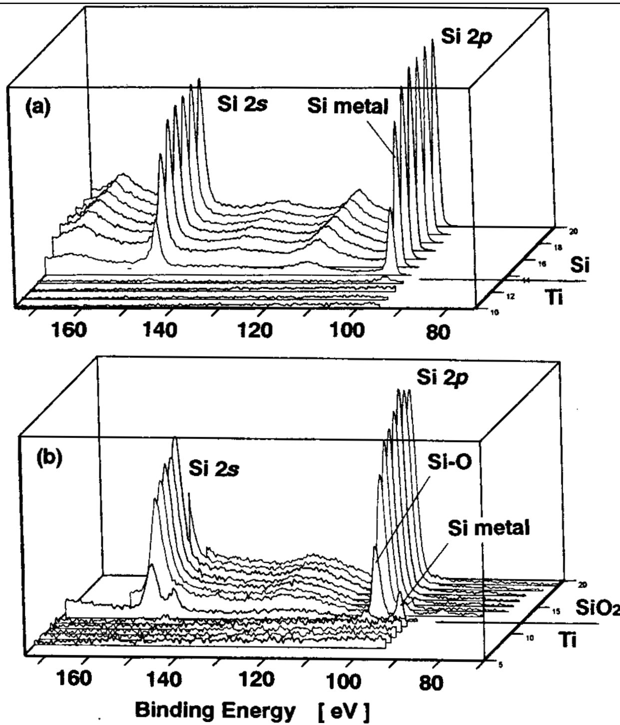

FIG. 6. XPS spectra for Si 2p near the boundary between (a) Ti and Si layers and (b) Ti and SiO_2 layers.

axes of Fig. 4 denote the detected signal intensity of atomic concentration in percent and the Ar ion etching time, respectively. The biggest difference in results between Figs. 4(a) and 4(b) was a concentration of oxygen (O) in the Ti layer. From the Ti film on the Si/SiO_2 [see Fig. 4 (a)], only a negligibly small concentration of O was found, whereas the Ti film directly deposited on the SiO_2 Iayer contained 8-10 atomic percents of O [see Fig. 4(b)]. Figure 4(a) also reveals that no oxygen was found in the Si layer on the SiO_2 , suggesting that the Si worked as an oxygen barrier for the Ti films in this sample.

Figure 5(a) shows photoelectron spectra for Ti 2p near the boundary between the Ti film and Si film. Figure 5(b) shows

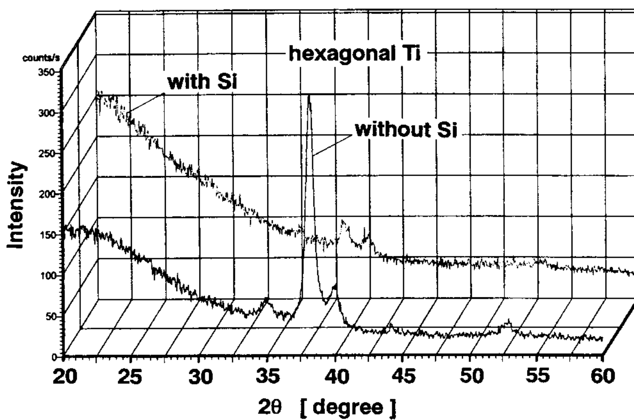

FIG. 7. A θ/26 XRD results for 50-nm-thick Ti films deposited on both Si/SiO_2 and SiO_2 layers The incidence angle of Cu $K\alpha$ x-ray beam was fixed at 1.2° from the sample surface to detect the signal from the thin layer.

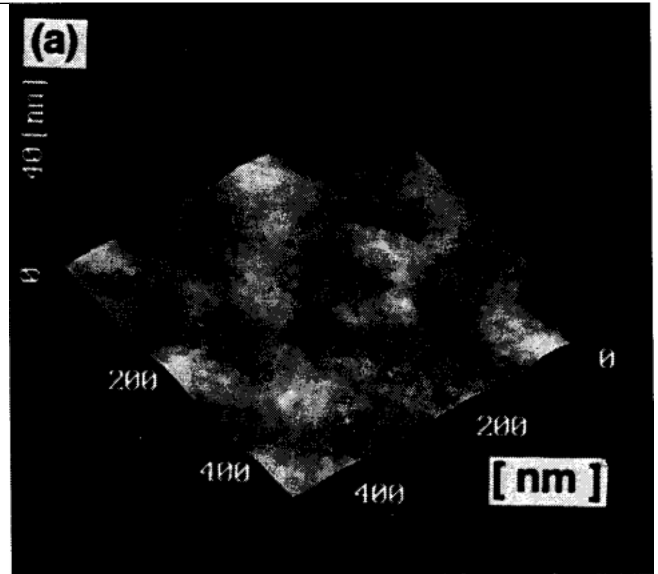

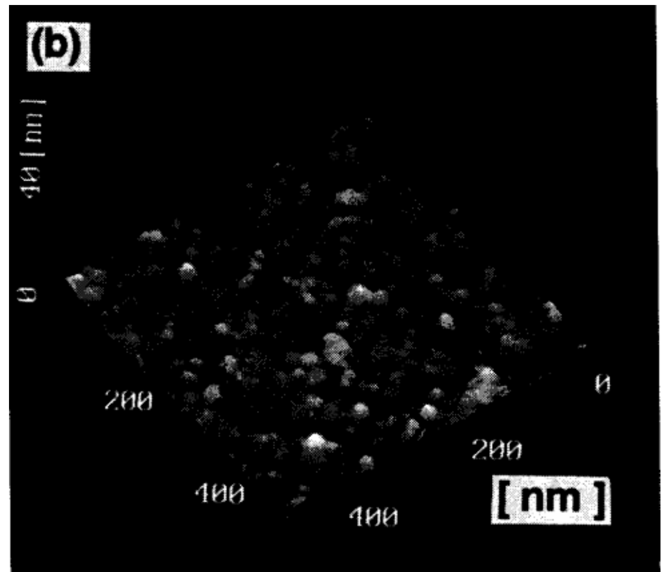

FIG. 8. AFM images observed on the suface of lO-nm-thick Ti films: (a) for the Ti films on SifSiO_2 and (b) for the Ti on SiO_2 -

similar spectra for the boundary between the Ti and SiO_2 - The horizontal axis of Fig. 5 denotes the measured binding energy which was calibrated using a certain C 1s peak energy. The spectra were measured at eleven different depth levels around the boundary. As shown in Fig. 5(a), on the Si coated SiO_2 , only a pair of Ti 2p peaks attributed to metallic Ti were observed throughout the boundary and film, indicating that the metallic Ti film grew successfully. However, from the boundary of the Ti film directly deposited on the SiO_2 Iayer, peaks due to oxidized Ti were found before peaks for metallic Ti appeared. Although the degree of oxidization through the Ti film, containing 8-10 atomic percents of oxygen as shown in Fig. 4(b), was not clarified in this measurement, a bottom layer of the deposited Ti film was chemically discontinuous and changed into metallic Ti from an oxidized Ti.

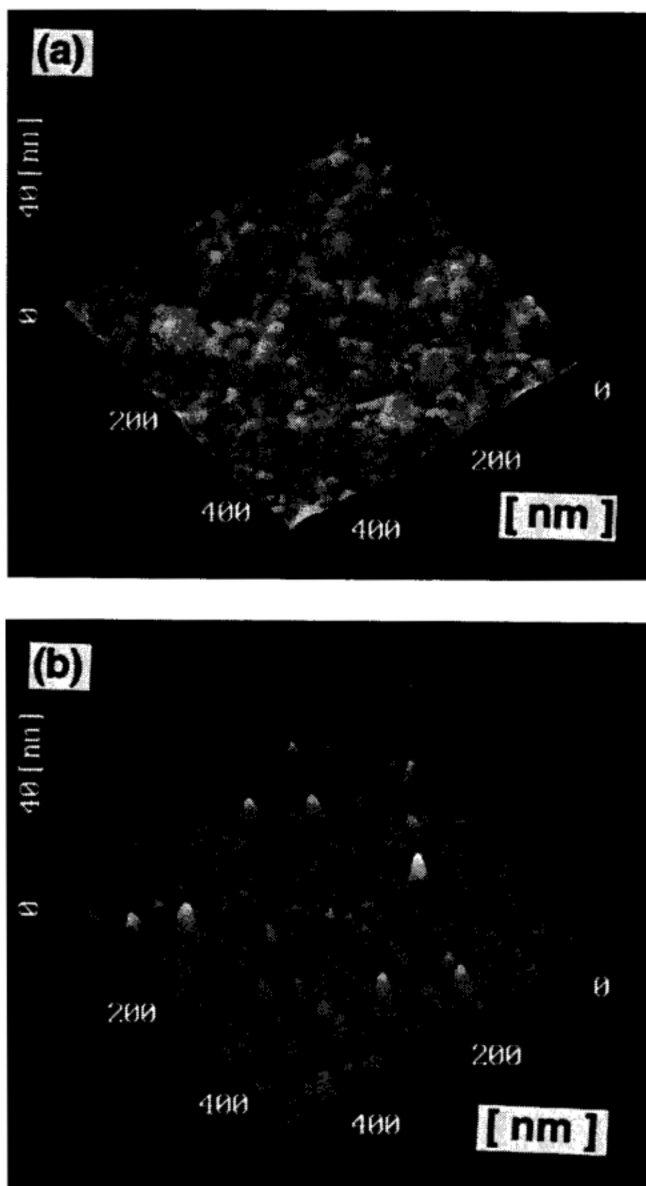

FIG. 9. AFM images observed on the surface of 50-nm-thick Ti films: (a) for the Ti films on SifSiO_2 and (b) for the Ti on SiO_2 -

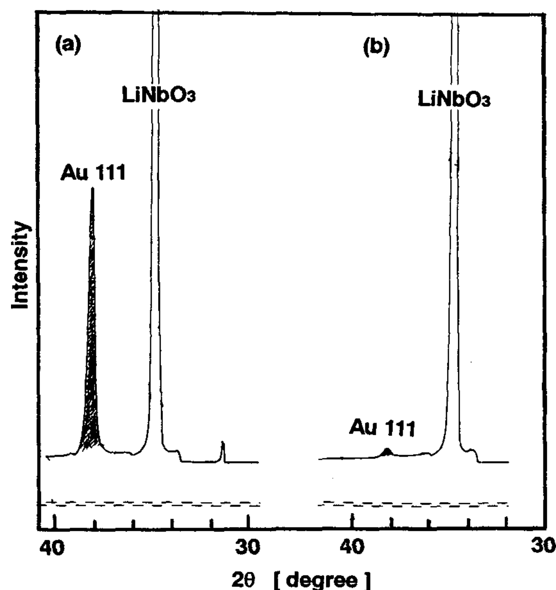

FIG. 10. A $\theta/2\theta$ XRD measurement result for the 35 nm thick Au layer on the Ti/Si/SiO_2 / $LiNbO_3$ (a) and on the Ti/SiO_2 / $LiNbO_3$(b).

Figures 6(a) and 6(b) are similar XPS results measured for Si 2*p* near the boundary with the Ti films. The Si spectra of Fig. 6(a) were caused by the Si film on the SiO_2 Iayer, and the chemical state of Si was found to be metal as expected. On the other hand, although all spectra of Fig. 6(b) should come from the SiO_2 and be attributed to oxidized Si, at the boundary with the Ti film, coexistence of the peak from metallic Si was found. The results indicated that a transportation of oxygen from the SiO_2 Iayer to the growing Ti film occurred at the boundary. Such consideration was supported by the fact that in a temperature vs oxygen potential diagram, the chemical equilibrium line for Si/SiO_2 reaction exists at the same level with the line for TiOfri$_2$O$_3$ reaction [6] Further, from the same diagram, the reaction from metallic Ti to TiO was known to occur more preferably than the oxidization of Si, suggesting that the Ti deposited on the SiO_2 took oxygen ions from the SiO_2 surface durin*' film growth.

We conclude that the Si film precoated on the SiO_2 layer acted as a preventative layer for the possible transportation of oxygen from the SiO_2 surface to the growing Ti. And, the existence of the oxidized Ti sublayer between the SiO_2 and Ti films was at least one cause leading to the weakness in their adhesive strength.

C. Physical Structure

Besides the partial oxidization in the Ti film on the SiO_2 without Si, grain growth of metallic Ti crystallites was found in the same sample. Figure 7 shows a $\theta/2\theta$ XRD results for 50-nm-thick Ti films deposited on both Si/SiO_2 and SiO_2 layers, in which the incidence angle of the Cu Ka x-ray beam was fixed at 1.2° from the sample surface to detect the signal from the thin layer. The observed peaks between $2\theta = 30°–40°$ were assigned to the diffraction from a metallic Ti structure (hexagonal structure). Furthermore, the observed peak intensity was larger in the sanrple without the Si inter layer, indicating an existence of larger crystallites (grains) in this thin Ti film sample.

The grain growth in the Ti film on the SiO_2 Was also detected by a direct observation of the film surface morphology through the AFM method. Figures 8 and 9 reveal AFM images observed for the surface of I O-nm- and 50-nm-thick Ti films, respectively; (a) is the result of the Ti film on Si/SiO_2 and (b) of the Ti on SiO_2 • As shown, the grain size was found to be larger in the Ti films directly deposited on the SiO_2 Without Si insertion. The grains of the 50-nm-thick Ti film grew larger, especially in height, than the grains in the lO-nm-thick film. On the Si/SiO_2 Iayer, the Ti film grew steadily, allowing grain size and surface flatness to remain consistent throughout its growth.

The partial oxidization of the growing Ti layer [see Fig. 4(b)] was thought to be one possible reason for larger grain growth in the Ti film on the SiO_2 • For instance, there was a

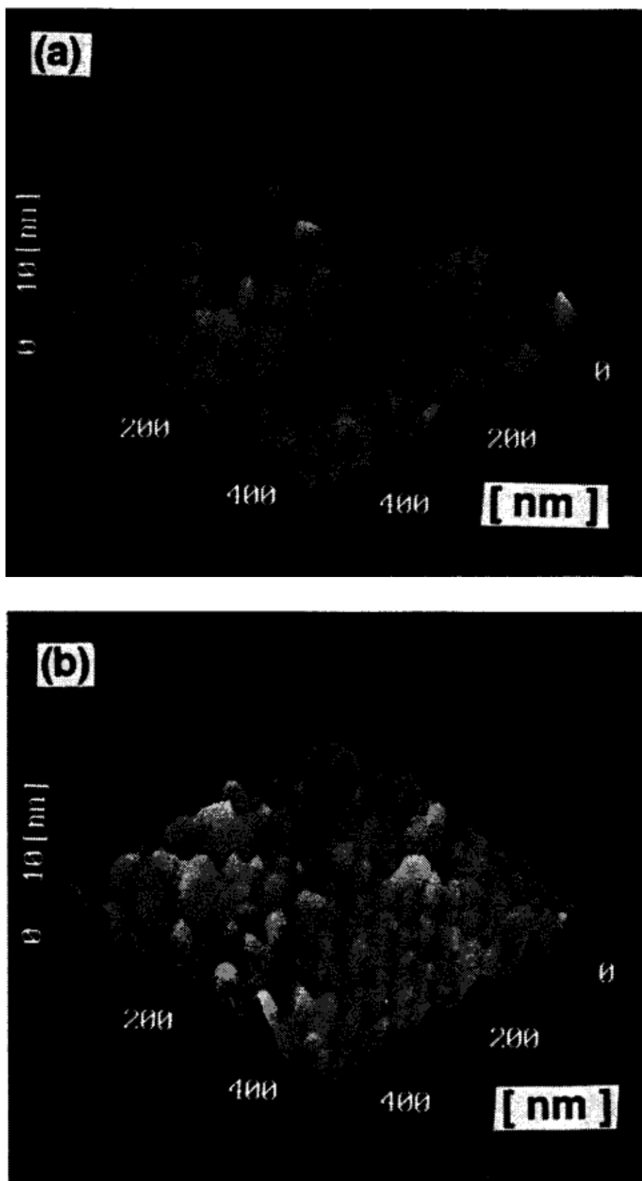

FIG. 11. AFM images of the 35 nm thick Au layer on the TifSVSiO$_2$/ LiNbO$_3$ (a) and on the Ti/SiO$_2$ / LiNbO$_3$ (b).

possibility that the titanium oxide layer initially formed on the SiO_2 [see Fig. 5(b)] introduced an inhomogeneous growth of metallic Ti crystallites due to the competing phase of oxidized Ti, resulting in rough surface growth. Furthermore, the oxidization throughout Ti film was thought to make the film fragile. In contrast, on the Si/SiO$_2$ surface, the fine Ti grains grew steadily and homogeneously, thus forming a smoother surface. However, an effect of the crystallinity of metallic Ti films on their mechanical strength was not sure in our experiments.

D. Effect of Ti layer on Structure of Au Covering Layer

As described above, the weak adhesive strength of the Au/Ti binary film on the SiO_2 Iayer may be due to oxidization of the Ti film. Furthermore, such anomaly in the Ti layer was found to infiuence the crystalline structure of the Au layer, although it had been prepared completely after the Ti deposition in the same evaporation deposition apparatus without breaking the vacuum.

Figure 10 shows a conventional $\theta/2\theta$ XRD measurement result for the 35-nm-thick Au layer on the Ti/Si/SiO$_2$ / LiNbO$_3$ (a) and on the Ti/SiO$_2$/LiNbO$_3$(b). Figures 11(a) and 1 1 (b) are the corresponding AFM images. On the metallic Ti film on the Si/SiO$_2$, the Au crystallites having preferential (111) orientation grew, but such growth was inferior in the other sample. Because the Ti suface fonned directly on the SiO_2 was rougher, a lateral coalescence of Au crystallites and their ultimate grain growth might be inferior compared with the Au film on the smooth Ti surface. Note that the observed structural difference of the Au layer did not seem to affect the performance of fabricated devices.

IV. CONCLUSIONS

Although the Ti layer was commonly used as an adhesive layer for the deposition of Au film on the SiO_2 Iayer, in our observation, the adhesive strength of the Ti to the vacuum evaporation deposited SiO_2 film was not high. The origin of such weakness may be oxidization of the growing Ti film due to oxygens transported from the SiO_2 • This reaction formed a thin layer composed of complete titanium oxides at the boundary and may induce stuctural discontinuity between the SiO_2 and metallic Ti layers. Further, oxidization throughout the Ti deposition process may cause inhomogeneous growth of metallic Ti crystallites and roughening of the surface. We concluded that the coexistence of an oxidized Ti in the film may make the film fragile, another factor for weak film bonding. In order to improve adnesive strength, the additional insertion of an Si layer between SiO_2 and Ti was proven to be effective. The Si layer prevented the oxidizing reaction between the SiO_2 and Ti films.

ACKNOWLEDGMENTS

This study was partially supported by Special Coordination Funds for Promoting Science and Technology "Fundamental research on new materials of function-harmonized oxides," from the Japanese Science and Technology Agency. The authors also thank gratefully Professor Baba of Seikei University for scratch tests and staff members of UBE Analysis Laboratory Co. for XPS measurements.

[1]For example; T. Sawaki and Shinku-Jyochaku, *Vacuum Evaporation*, 4th ed. (Nikkan Kogyo Shinbun, Tokyo, Japan, 1969), Chaps. 7, 8 (in Japanese).
[2]H. Nagata and J. Ichikawa. Opt. Eng (Bellingham) **34**, 3284 (1995).
[3]M. A. Powell and A. O'Donnell. Opt. Photonics News **8**, 23 (1997).
[4]R. S. Moyer, R. Grencavich, R. W. Smith, and W. J. Minford, *Proceedings of Electronic Component and Technology Conference, May 18-21, 1997, San Jose* (IEEE. New York, 1997), p. 425.
[5]A. Kikuchi. S. Baba. and A. Kinbara, Vacuum **2**, 68 (1989) (in Japanese)
[6]Denkikagaku-Binran, *Handbook of Electrochemistry*, 4th ed , edited by K. Fueki (Maruzen. Tokyo, 1985). Chap. 2.